

Effect of ultrasonic irradiation and TiO₂ on the determination of electrical and dielectric properties of PEO–P(VdF-HFP)–LiClO₄-based nanocomposite polymer blend electrolytes

S. Jayanthi · B. Sundaresan

Received: 13 June 2014 / Revised: 4 August 2014 / Accepted: 7 August 2014 / Published online: 31 August 2014
© Springer-Verlag Berlin Heidelberg 2014

Abstract Nanocomposite polymer blend electrolytes composed of PEO–P(VdF-HFP)–LiClO₄ were prepared for various concentrations of TiO₂ nanofiller. All the composite electrolytes were subjected to ultrasonic irradiation for enhancing the ionic conductivity of the composite electrolytes. It was noted that the ultrasonic irradiated samples exhibited a higher ionic conductivity than the non-irradiated samples. In addition, filler concentration in the complex was also optimized based on ionic conductivity, and it was noted that the sample containing 6 wt% showed maximum value about $1.451 \times 10^{-5} \text{ S cm}^{-1}$; however, this is lower than the value obtained from the irradiated samples ($2.27 \times 10^{-4} \text{ S cm}^{-1}$). The dielectric, modulus and tangent loss behaviour of the samples were also estimated and discussed. Thermal and surface images studies were also carried out using TG/DTA and AFM studies, respectively. In addition, mobility and diffusion coefficient characteristics were also evaluated.

Keywords AC conductivities · Li⁺ conductors · Composite electrolytes · Electrochemical characterizations · Polymer electrolytes

Introduction

Solid polymer electrolytes (SPEs) have received great attention due to their potential applications in various electrochemical devices such as rechargeable Li-ion batteries, electrochemical super capacitors, electrochromic display devices and etc. [1–3]. Solid polymer electrolytes were prepared using

different polymer hosts for achieving high conductivity and thermal and mechanical stability. Among the polymer hosts, polyethylene oxide (PEO)-based SPEs have been extensively studied due to its high ionic conductivity of the order of 10^{-3} – $10^{-4} \text{ S cm}^{-1}$ at high temperature in the range of 80–100 °C [4]; however, due to the high crystalline nature of PEO, the polymer electrolytes showed poor room temperature ionic conductivity of the order of 10^{-7} – $10^{-8} \text{ S cm}^{-1}$ [5]. So far, various approaches have been carried on PEO-based polymer electrolytes in order to increase the ambient temperature ionic conductivity of the system. Among the different approaches, the most common method is the addition of high dielectric low-range molecule called plasticizers to the polymer matrix. This plasticized polymer matrix exhibits higher ionic conductivity of the order of $10^{-3} \text{ S cm}^{-1}$. However, these plasticized electrolytes could not be used as a promising candidate in device fabrications due to their drawbacks such as solvent volatility, increased reactivity with lithium metal electrode and poor mechanical properties at high degree of polarization [6]. On the other hand, polymer electrolytes have been prepared using two or more polymers called polymer blends for improving the ionic conductivity and mechanical strength of the polymer electrolytes. Blending of polymers has many advantages over other techniques such as easy preparation and control of the physical properties within the miscibility compositional regime [7]. Among the various polymer blends studied, poly(ethylene oxide) (PEO)/poly(vinylidene fluoride-co-hexafluoropropylene) P(VdF-co-HFP) have attracted many researchers because of its good compatible nature, high mechanical stability and support to the ion transport [8]. Apart from the above-method of preparations, ionic conductivity of SPEs has also been enhanced by dispersing nanosized ceramic filler [9]; it was believed that the addition of the nanofiller into the polymer matrix showed an appreciable conductivity than the other kind of electrolyte systems which is due to the interactions of chain segments with the acid sites of the filler;

S. Jayanthi · B. Sundaresan (✉)
Centre for Research and Post-Graduate Studies in Physics,
Ayya Nadar Janaki Ammal College (Autonomous),
Sivakasi 626 124, Tamil Nadu, India
e-mail: bs.journals@gmail.com

as a result, the lithium-ion mobility of the electrolyte system was enhanced further [10]. Hence, in the present work, an attempt has been made on PEO–P(VdF-co-HFP)-based blend electrolyte. The choice of choosing the copolymer P(VdF-HFP) is because of its more appealing properties such as high dielectric constant ($\epsilon=8.4$), glass transition temperature and low crystallinity. Further, it possesses excellent chemical stability due to VdF unit and plasticity due to HFP unit [8]. The ether coordination site of PEO makes the polymer more polar and facilitates for the dissociation of the given salts for ion transport to take place, which is responsible for the higher ionic conductivity of the polymer electrolyte system. Furthermore, PEO also has high electrochemical stability [11]; hence, it has been used as one of the polymer hosts.

In order to facilitate the higher degree of ionization of the salt, low lattice energy is considered as an important criterion. Hence, in the present investigation, LiClO₄ have been chosen as the ionic salt because of its low lattice energy of 723 KJ mol⁻¹, high thermal stability and less hygroscopicity which facilitate for increasing charge carriers [12] in the polymer electrolyte matrix. In the present work, the polymer blend electrolytes based on the blend of PEO/PVdF-co-HFP with fixed ratio of LiClO₄ have been prepared for various concentrations of TiO₂ nanofiller. Prepared polymer electrolytes have been subjected to different physical characterizations and electrochemical impedance spectroscopic studies in order to define their structural and electric properties, respectively. Ionic conductivity of the polymer blend electrolyte has been optimized by varying the TiO₂ content and by tuning the sonication time of the ultrasonic irradiation experiment. The optimum value of ultrasonic irradiation time is determined with a view to prepare efficient nanocomposite polymer blend electrolytes (NCPBEs) with enhancement in electrical and dielectric properties.

Experimental

Materials and methods

PEO (Mw~8×10⁶ g mol⁻¹), P(VdF-HFP) (Mw~130×10³ g mol⁻¹) and LiClO₄ were obtained from Aldrich, USA, and used in the present study. Nanosized TiO₂ with an average size of 27.03 nm was procured from Alfa Aeson, India. The solvent acetonitrile was purchased from Merck, India. All the above said chemicals were used without any further purification. Ultrasonic generator (Model PR 1000MP, Oscar Ultrasonic, Mumbai) giving a power output and frequency of 1,000 W and 20 KHz, respectively, along with a titanium horn of diameter 6 mm was used for irradiation.

Preparation of nanocomposite polymer blend electrolytes

Thick films of PEO–P(VdF-HFP)–LiClO₄ with TiO₂ in different weight ratios (2 to 10 wt%) were prepared by solvent-casting technique using conventional mechanical stirring and ultrasonic irradiation methods. The composition of polymers and salt was fixed as PEO (20 wt%)–P(VdF-HFP) (50 wt%)–LiClO₄ (30 wt%) as it was found to be an optimized composition. The above said quantities of PEO, P(VdF-HFP) and LiClO₄ were dissolved by adding acetonitrile in sequence to the solvent and stirred well for 24 h. Then, the inorganic nanofiller TiO₂ (27.03 nm) at various compositions from 2 to 10 wt% (insteps of 2 wt%) was suspended in the solution and stirred well for 24 h until a homogenous solution was obtained. After blending the compound well, ultrasonic irradiation was carried out with the probe of the ultrasonic horn immersed in the polymer matrix. In order to study the effect of ultrasonic irradiation time on the properties of the samples, the ultrasonic irradiation was carried out for different durations, say 5, 10, 15 and 20 mins. The obtained solutions were then casted on to a Teflon dish and kept in a vacuum oven at 65 °C at a pressure of 10⁻³ Torr for 2 days so as to remove any traces of solvent. This procedure yields mechanically stable and free-standing films.

Characterization techniques

AC impedance analysis

Impedance values of the NCPBEs were determined with the help of stainless steel electrodes using PSM1735 impedance analyzer supplied by Newton's 4th Ltd., UK. The samples were sandwiched between two stainless steel (SS) electrodes with signal amplitude of 2 mV, and the operating frequency range was 1 to 10 MHz. All the measurements were carried out in the temperature range 303–353 K.

Dielectric studies

The dielectric constant ϵ' and the dielectric loss ϵ'' can be defined as follows:

$$\epsilon'(\omega) = \frac{z''}{\omega C_o (Z'^2 + Z''^2)} \quad (1)$$

$$\epsilon''(\omega) = \frac{z'}{\omega C_o (Z'^2 + Z''^2)} \quad (2)$$

where z' represents the real impedance, z'' represents the imaginary impedance, ω is the angular frequency, C_o represents the vacuum capacitance, ϵ' is the real permittivity and ϵ'' is the imaginary permittivity.

The real and imaginary parts of the electrical modulus M' and imaginary parts of the electrical modulus were calculated from the following:

$$M'(\omega) = \frac{\varepsilon'}{(\varepsilon'^2 + \varepsilon''^2)} \quad (3)$$

$$M''(\omega) = \frac{\varepsilon''}{(\varepsilon'^2 + \varepsilon''^2)} \quad (4)$$

The tangent loss can be expressed as

$$\tan\delta = \frac{\varepsilon''}{\varepsilon'} \text{ (or) } \frac{M''}{M'} \quad (5)$$

Out of the above electric and dielectrical analysis, polymer electrolytes have also been subjected to AFM surface image studies. The 3D AFM images were depicted using Agilent Pico LE microscope.

TGA 2950 model was used to characterize the thermal stability of the nanocomposite polymer electrolyte. Approximately 10 mg of sample was cut into minute pieces and loaded onto a platinum pan before insertion into the TGA furnace and purged with nitrogen gas. A temperature ramp of 20 °C/min from approximately room temperature to 600 °C was programmed.

Results and discussion

Ionic conductivity

Complex ac impedance plot of PEO–P(VdF–HFP)–LiClO₄–TiO₂ (X wt%) (where $X=0, 2, 4, 6, 8$ and 10) electrolytes prepared via the conventional mechanical stirring is given in Fig. 1a. These plots show a semicircle in the high-frequency region and a spike in the low-frequency region. The high-frequency semicircle is due to the parallel combination of a resistor and capacitor, whereas the spike in the low-frequency region is due to the formation of double-layer capacitance at the electrode–electrolyte interface. Further, the spike is inclined at an angle less than 90°. This is due to the inhomogeneous nature of the electrode–electrolyte interface [13].

The ionic conductivity of NCPBEs is calculated from the following equation:

$$\sigma = \frac{l}{AR_B} \quad (6)$$

where l is the thickness of the sample, A the area of the electrolyte sample used and R_B the bulk resistance. Intercept

of the low-frequency spike at the real axis of the complex impedance plot gives the value of R_B .

Plot of ionic conductivity Vs TiO₂ concentration of the electrolytes prepared using conventional mechanical stirring is shown in Fig. 1b. It is observed that the ionic conductivity increased with respect to the TiO₂ concentration up to 6 wt% and then it decreased for the further addition of 8 wt% of TiO₂ concentration. Maximum value of ionic conductivity is obtained as 1.451×10^{-5} S cm⁻¹ for 6 wt% TiO₂ added system which is greater in two orders of magnitude when compared with the value 9.570×10^{-7} S cm⁻¹ of TiO₂ free system. This enhancement of ionic conductivity is due to the formation of amorphous domains which results in the strong interaction of filler particles with polymer chains [14]. The obtained ionic conductivity is well correlated with the values obtained by Rajendran et al. [8].

Thus, the enhancement of ionic conductivity results from Lewis acid–base reactions between the TiO₂ nanoparticle and the PEO–P(VdF–HFP) segments. Similar effect was observed for PEO–P(VdF–HFP)–Al₂O₃–based composite electrolyte system by Liao et al. [14]. Nano TiO₂ competes with lithium cations as Lewis acid for the formation of complexes of PEO–P(VdF–HFP). Thus, the nanoparticle acts as cross-linking centres for the polymer segments, lowering the polymer chain reorganization tendency and promoting an overall structure stiffness. Such a structure modification provides lithium ion conducting pathways at the high surface area of the nanoparticles and shortens the Li⁺ ion transport distance. The interactions of Lewis acidic TiO₂ with ClO₄⁻ anions lead to the liberation of higher amounts of free Li⁺ which is also responsible for the increase of ionic conductivity against the concentration of TiO₂. The polymer electrolyte system at low filler compositions may be imagined as a conducting medium where filler grains are randomly and uniformly distributed throughout the volume. This would give rise to additional favourable conducting pathways in the vicinity of the surface of the grains, which could account for the observed increase in ionic conductivity [15].

The Lewis acid–base interactions of TiO₂ with PEO–P(VdF–HFP) blends and ClO₄⁻ anions seem to be less pronounced when the content of TiO₂ is higher than 6 wt%. This may be due to the enhancement of TiO₂–TiO₂ interactions over the Lewis acid–base interactions at higher concentrations of TiO₂. Further, when the filler concentration is increased, the filler grains get close enough to each other, such that the geometrical constrictions imposed by the more abundant nanofiller TiO₂ grains become large. This enables the long polymer chains to become more immobilized, leading to a lower ionic conductivity [15]. Thus, the conductivity reaches a maximum at low filler concentrations followed by a subsequent drop at the high filler concentrations (Fig. 1b).

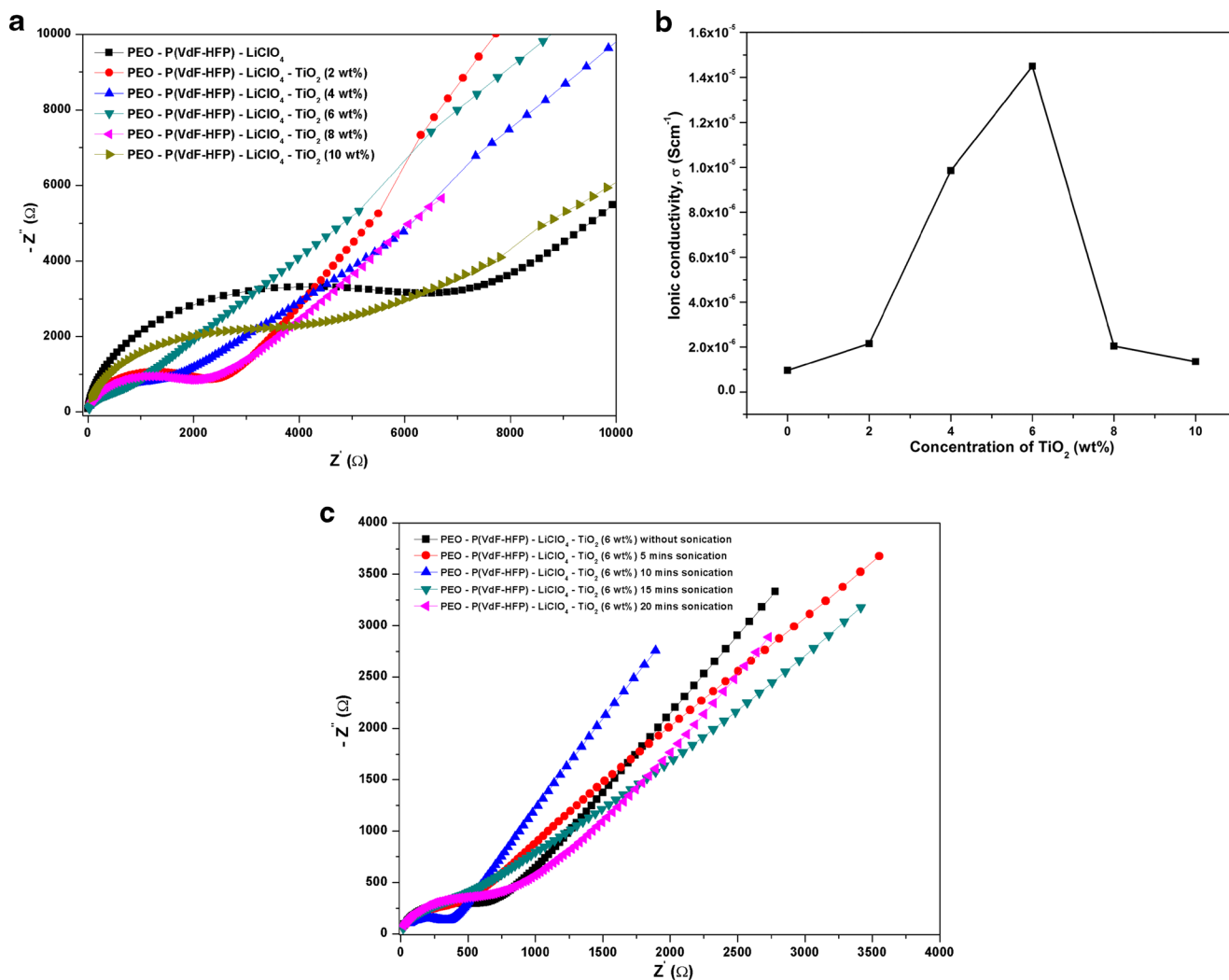


Fig. 1 **a** AC impedance plot of NCPBEs prepared through conventional mechanical stirring at room temperature. **b** Ionic conductivity Vs concentration plot of the NCPBEs prepared through conventional mechanical

stirring. **c** impedance plot of 6 wt% TiO₂ added NCPBE for the different durations of ultrasonic irradiation

Effect of ultrasonic irradiation on the ionic conductivity of NCPBEs

Appropriate ultrasonic irradiation helps to improve the amorphous region of the polymer electrolyte; hence, the ionic conductivity of the samples was enhanced further [16]. The AC impedance plot of the sample (6 wt% of TiO₂ added system) exhibiting a maximum ionic conductivity for various durations of ultrasonic irradiation is shown in Fig. 1c. For a better understanding, electrolytes with different concentrations of TiO₂ are also subjected to ultrasonic irradiation at different time durations; the obtained ionic conductivity values are given in Table 1. It can be seen from Table 1 that the effect of ultrasonic irradiation plays a significant role in the determination of ionic conductivity, and it is varied with respect to the sonication time from 5 to 20 mins with a constant time interval of 5 mins. The optimum ultrasonic irradiation time to achieve the maximum ionic conductivity

is found to be different for different concentrations of TiO₂-based system. It is 15 mins for 2 wt% of TiO₂, 5 mins for 4 wt% of TiO₂, 10 mins for 6 wt% of TiO₂ and 5 mins for 8 wt% of TiO₂ added systems. At 10 wt% of TiO₂, there is no significant increase in ionic conductivity. However, other concentrations from 2 to 8 wt% showed an enhanced ionic conductivity by an order of magnitude for the aforementioned optimum ultrasonic irradiation time.

Overall, the maximum value of ionic conductivity, $22.70 \times 10^{-5} \text{ Scm}^{-1}$, is obtained for 6 wt% TiO₂ added system at an appropriate ultrasonic irradiation time of 10 mins; this value is higher than the conductivity value $1.451 \times 10^{-5} \text{ S cm}^{-1}$ obtained from the conventional mechanical stirring method for the 6 wt% TiO₂ added system. It indicated that the increase in ionic conductivity with optimum ultrasonic irradiation time is due to the homogenous dispersion of TiO₂ nanoparticles in the viscous polymer blend which in turn facilitates the better migration of ions. However, at a higher TiO₂ concentration

Table 1 Room temperature ionic conductivity value of the samples prepared using conventional mechanical stirring and ultrasonic irradiations

Sample Code	Sample compositions PEO (20 wt%)-P(VdF-HFP) (50 wt%)-LiClO ₄ (30 wt%) TiO ₂ (<i>X</i> wt.%)	Room temperature ionic conductivity of the sample prepared by mechanical stirring ×10 ⁻⁵ S cm ⁻¹	Room temperature ionic conductivity at different ultra sonication times ×10 ⁻⁵ S cm ⁻¹			
			5 mins	10 mins	15 mins	20 mins
T1	<i>X</i> =2	0.2153	0.4850	0.6571	1.0080	0.2700
T2	<i>X</i> =4	0.9855	2.7640	0.2335	0.1718	0.0361
T3	<i>X</i> =6	<i>1.4510</i>	<i>5.0760</i>	<i>22.700</i>	<i>0.9990</i>	<i>0.8647</i>
T4	<i>X</i> =8	0.2042	1.4950	0.9986	0.3281	0.1550
T5	<i>X</i> =10	0.1354	0.1519	0.2206	0.1718	0.1152

Values in italic correspond to the enhanced ionic conductivity

(10 wt %), there is no significant increase in ionic conductivity which reveals that the ultrasonic irradiation does not help in obtaining a homogenous dispersion of TiO₂ at the higher concentration. The agglomeration of TiO₂ at the higher concentration leads to a cluster which is not destroyed by the ultrasonic irradiation, and hence, the cluster does not permit Li⁺ ions properly to move within the polymer electrolyte. Hence, it is noted that the optimum ultrasonic irradiation and the filler concentration is about 10 mins and 6 wt % of TiO₂, respectively, for PEO–P(VdF-HFP)–LiClO₄–TiO₂ system which exhibited a maximum ionic conductivity.

Evaluation of mobility, number of charge carriers and diffusion coefficient

Conductivity of the sample can also be represented as

$$\sigma = nq\mu \tag{7}$$

where ‘*n*’ is the number of mobile charge carriers; ‘*μ*’ is the mobility and diffusion coefficient ‘*D*’.

Mobility (*μ*) of the system is expressed as

$$\mu = \frac{qL^2}{4M\tau_{ep}KT} \tag{8}$$

where *q* is the charge on the carrier, *L* is the sample thickness, *M* is defined as the ratio of the sample thickness to twice the Debye length and τ_{ep} is relaxation in the presence of polarization [17].

M and τ_{ep} are correlated with tan δ as

$$\tan \delta = \frac{\omega\tau_{ep}}{1 + \omega^2\left(\tau_{ep}^2/M\right)} \tag{9}$$

The diffusion coefficient can be obtained using the Einstein relation

$$D = (KT/e)/\mu \tag{10}$$

where *K* is the Boltzmann constant, *e* is the elementary charge and *T* is the absolute temperature.

Ion concentration is determined as

$$n = (\sigma/D)(KT/e^2) \tag{11}$$

The values of *n*, *μ* and *D* are obtained for PEO–P(VdF-co-HFP)–LiClO₄–TiO₂ (6 wt%) prepared by both conventional mechanical stirring, and the optimum ultrasonic irradiation time of 10 mins are given in Table 2. The values of the later system are found to be higher than that of the former system.

This increase in ‘*n*’ would be due to the availability of loosely entangled Li⁺ ions with the polymer chains, while the increase in ‘*μ*’ and ‘*D*’ would be a consequence of increased degree of amorphousity of the prepared samples. The significant increase of the above values reveals that the ion-conducting behaviour of the samples is enhanced due to ultrasonic irradiation of the solution. It is also revealed that the Li⁺ ion is being the sole charge carriers in the samples [18].

Temperature dependence of the ionic conductivity

A study of the literature on SPEs of several electrolytes suggests Arrhenius as well as non-Arrhenius or Vogel–Tamman–Fulcher (VTF) types of ionic conduction which depends on the type of the additives, polymer and temperature range [19]. Figure 2 shows the variation of log σ with inverse absolute temperature for the systems PEO–P(VdF-HFP)–LiClO₄ and PEO–P(VdF-HFP)–LiClO₄–TiO₂ (6 wt%) prepared by both conventional mechanical stirring and the optimum ultrasonic irradiation for 10 mins. Absence of any abrupt jump of log σ with temperature in Fig. 2 indicates that these systems exhibit an amorphous structure [20]. The observed increase in ionic conductivity with the increase of temperature is ascribed to the decrease in viscosity and hence to the increased chain flexibility [21]. When the temperature increases, ions solvated molecules or polymer segment can move into the free volume [22]. The segmental motion will

Table 2 Mobility, diffusion coefficient, ion concentration of the prepared samples

Sample code	Properties of the prepared samples by conventional mechanical stirring			Properties of the prepared sample (T3) after 10 mins of ultrasonic irradiation		
	Mobility (μ) $\text{Cm}^2\text{V}^{-1}\text{S}^{-1}$	Diffusion coefficient (D) cm^2/S	n cm^{-3}	Mobility (μ) $\text{Cm}^2\text{V}^{-1}\text{S}^{-1}$	Diffusion coefficient (D) cm^2/S	n cm^{-3}
T1	7.110×10^{-2}	1.788×10^{-3}	1.373×10^{15}	–	–	–
T2	19.450×10^{-2}	4.891×10^{-3}	4.808×10^{15}	–	–	–
T3	<i>26.532×10^{-2}</i>	<i>6.672×10^{-3}</i>	<i>5.860×10^{15}</i>	<i>54.836×10^{-2}</i>	<i>1.379×10^{-2}</i>	<i>3.525×10^{14}</i>
T4	8.154×10^{-3}	2.050×10^{-3}	1.153×10^{14}	–	–	–
T5	3.401×10^{-3}	8.553×10^{-4}	1.021×10^{14}	–	–	–

Values in italic correspond to the enhanced mobility, diffusion coefficient and ion concentration

either allow the ions to hop from one site to another or provide an alternative for ions to move. Thus, the segmental movement of the PEO and P(VdF-HFP) facilitates the transitional ionic motion [1].

As the amorphous region increases, the polymer chain needs faster internal modes in which bond rotation creates segmental motion to favour inter and intra chain ion hopping. This in turn increases the ionic conductivity [23].

The ionic conductivity of the prepared systems can be expressed as

$$\sigma(T) = \sigma_0 \exp\left[\frac{-E_a}{KT}\right] \quad (12)$$

where σ_0 is the conductivity pre-exponential factor and E_a is the activation energy for conduction. By the least-square method, the activation energy for the systems was determined and the values are given in Table 3. According to Nookala et al. [24], the energy required for Li^+ ion to cross the barrier is a function of energy required for the reorganization of molecules.

E_a value is 0.872 eV for the system PEO–P(VdF-HFP)– LiClO_4 . It is 0.459 and 0.384 eV for the systems with TiO_2 (6 wt%) prepared through both the conventional mechanical

stirring and ultrasonic irradiation methods, respectively. The decreased E_a value, 0.384 eV, of the later system suggests that, after the optimum ultrasonic irradiation, the nano TiO_2 particles can better facilitate the migration of ions. According to Druger et al. [25], the change in conductivity with temperature in SPEs can be explained by the increase in the free volume of the system which improves the migration of ions. For devices, to operate over a wide temperature range, it is desirable to have a maximum ionic conductivity. Thus, systems with the low values of activation energies are desirable [26]. Hence, the prepared NCPBEs prepared using ultrasonic irradiation in the present work show promise for application in Li batteries over a wide temperature range.

Frequency-dependent conductivity

In order to explore the ion transport mechanism, the conductivity is calculated as a function of frequency from the real and imaginary parts of the impedance data. Figure 3a shows the frequency-dependent conductivity spectra of NCPBEs prepared through conventional mechanical stirring whereas Fig. 3b shows the said spectra for the system PEO–P(VdF-HFP)– LiClO_4 – TiO_2 (6 wt%) prepared using ultrasonic irradiation. It is observed from both figures that the frequency dependence of conductivity spectra shows two regimes, (1) the low-frequency plateau region and (2) the high-frequency dispersion region. The low-frequency plateau region corresponds to the frequency-independent conductivity σ_0 (or) σ_{dc} . The value of σ_0 is obtained by extrapolating the plateau to the lower frequency. The frequency dependence of conductivity in the high-frequency dispersion region is analysed using the universal Johnson's power law relation [27]

$$\sigma(\omega) = \sigma_0 + A\omega^n \quad (13)$$

where σ_0 is the limiting zero frequency conductivity and A is the pre-exponential constant, ω is the angular frequency and n is the power law exponent where $0 < n < 1$. Using the above equation, the fitting parameters σ_0 , A and n are obtained and are given in Tables 4 and 5.

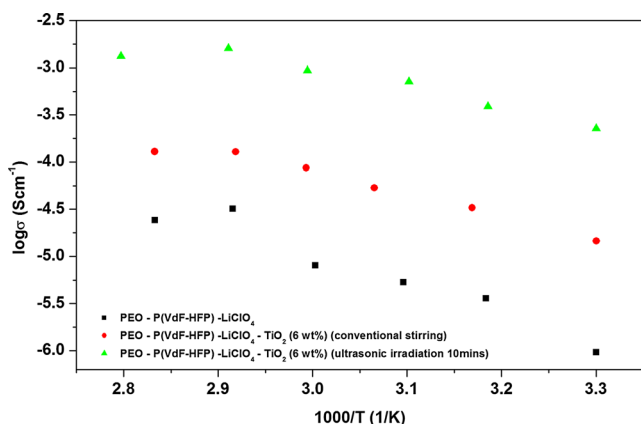


Fig. 2 Variation of $\log \sigma$ with inverse absolute temperature for the prepared systems

Table 3 Comparison of the activation energy of the prepared samples

Sample code	σ_0 S cm ⁻¹	Ea (eV)
PEO–P(VdF–HFP)–LiClO ₄	9.567×10 ⁻⁷	0.872
PEO–P(VdF–HFP)–LiClO ₄ –TiO ₂ (6 wt%)	1.451×10 ⁻⁵	0.459
PEO–P(VdF–HFP)–LiClO ₄ –TiO ₂ (6 wt%) (ultrasonic irradiation time of 10 mins)	2.270×10 ⁻⁴	0.384

The values of σ_0 obtained from the Jonscher’s power law relation are found to slightly different from the conductivity obtained from the Cole–Cole plot. This variation of conductivity is reflected in the mechanism of charge transport and interactions among the charge carriers. According to the Jump relaxation model [28], at low frequencies, ions jump from one site to its neighbouring vacant site, while at higher frequencies, due to the short time periods, the probability for ions to go fall back to their original site increases and more hopping of ions is responsible for the higher conductivity in lower frequencies.

The power law exponent ‘*n*’ relates the back hop rate to the site relaxation time [34]

$$n = \text{back hop rate/site relaxation time}$$

If *n* is less than one, the backward hopping is slower than the site relaxation. It results in the translational motion of Li⁺ ion. But if the value of *n* is >1, then the backward hopping is faster than the site relaxation time. In the present study, *n* values are less than one which indicates that the backward hopping is slower than the site relaxation. Further, it has been stated that the low values of *n* (*n*<1) are due to the formation of free sites for Li⁺ ion transport [29].

The hopping frequency of the charge carriers (ω_p) can be estimated by the following equation [30].

$$\omega_p = \left(\frac{\sigma_0}{A}\right)^{\frac{1}{n}} \tag{14}$$

The values of ω_p for the system prepared through conventional mechanical stirring and the system prepared through an optimum irradiation time of 10 mins are given in Tables 4 and 5. The values of ω_p decreased with the addition of nano TiO₂ for the system prepared through conventional mechanical stirring (Table 4). This indicates that the mobility of ions has been enhanced after the incorporation of nano TiO₂ into the polymer blend matrix.

ω_p is 6.562×10³ for the sample, prepared with an optimum ultrasonic irradiation time of 10 mins (Table 5), which is three orders of magnitude lesser than the sample prepared through conventional mechanical stirring. It suggests that the mobility of ions has further been enhanced when the ultrasonic irradiation method is adopted.

Dielectric analysis

Figure 4a, b shows the frequency dependence of the dielectric constant ϵ' and dielectric loss ϵ'' for the prepared NCPBE using conventional mechanical stirring, whereas Fig. 4c, d is of the system prepared at different ultrasonic irradiation times.

No appreciable relaxation peaks are observed in the above said figures. It indicates that the increase in ionic conductivity is primarily due to an increase in the number density of mobile ions. The values of ϵ' are given in Table 4. It is observed from the tables that the value of ϵ' increases due to the addition of nanofiller TiO₂ and also due to ultrasonic irradiation. This increase in the value of ϵ' indicates that the charge carrier density at the electrode–electrolyte interface has been

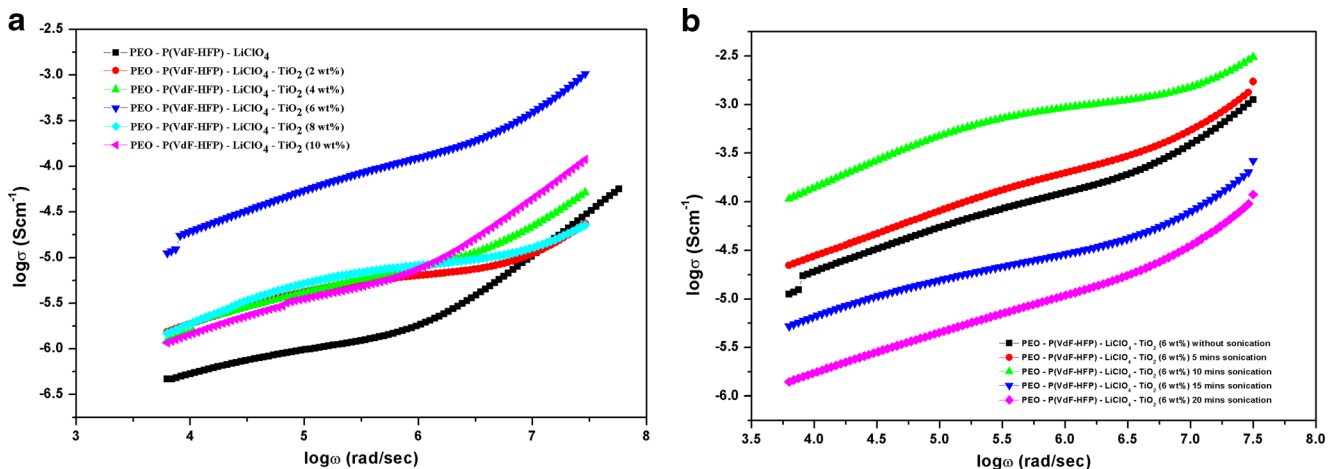


Fig. 3 a Frequency-dependent conductivity spectra of NCPBEs (conventional mechanical stirring). b Frequency-dependent conductivity spectra for the system PEO–P(VdF–HFP)–LiClO₄–TiO₂ (6 wt%) at different ultrasonic irradiation times

Table 4 Dielectric parameters σ_0 , A , n , ω_p , ε' , β and τ for the NCPBEs prepared using mechanical stirring

Concentration of TiO ₂ (wt%)	σ (S cm ⁻¹) (from cole–cole plot)	σ_0 (S cm ⁻¹) (from Jonscher's power law fit)	A	n	ω_p	ε' (at 1 KHz)	β	τ (s)
0	9.567×10^{-7}	4.633×10^{-7}	1.327×10^{-12}	0.983	0.435×10^6	2.268	0.765	7.450×10^{-4}
2	2.153×10^{-6}	1.563×10^{-6}	1.403×10^{-9}	0.554	0.316×10^6	6.987	0.689	1.125×10^{-5}
4	9.855×10^{-6}	1.264×10^{-6}	3.578×10^{-10}	0.684	0.153×10^6	8.762	0.824	3.405×10^{-5}
6	1.451×10^{-5}	1.000×10^{-5}	3.995×10^{-9}	0.715	0.056×10^6	21.124	0.762	2.692×10^{-5}
8	2.042×10^{-6}	1.505×10^{-6}	3.080×10^{-8}	0.371	0.035×10^6	11.845	0.782	7.536×10^{-6}
10	1.354×10^{-6}	1.186×10^{-6}	1.427×10^{-11}	0.927	0.202×10^6	5.955	0.693	8.495×10^{-5}

enhanced which results in the increase of equivalent capacitance [31].

It is also observed from the plots of ε' and ε'' that the values of ε' and ε'' are high in the low-frequency region followed by a rapid decrease and reaches a constant value in the higher-frequency side. This variation is attributed to the tendency of dipoles in the macromolecules to orient themselves in the direction of the applied field within the low-frequency range. But, in the higher-frequency side, the dipoles are unable to orient themselves in the direction of the applied field and hence the values of ε' and ε'' decrease [32]. A sharp increase of ε' and ε'' towards lower-frequency side is due to the presence of electrode polarization effects [33]. Thus, the addition of nanofiller TiO₂ is expected to increase the degree of salt dissociation and redissociation, which increases the number of mobile Li⁺.

The observed variations in ε' and ε'' with frequency is attributed to the formation of space charge region at the electrode–electrolyte interface, which is known as $\omega^{(n-1)}$ variation or the non-Debye behaviour. This implies that the conductivity exhibits relaxation, which is non-exponential in time [34]. It indicates the existence of space charge polarization, where there is time for charges to build up at the interface before the applied field changes direction, giving larger values of ε' and ε'' . On the other hand, there is no time for charge build-up at the interface with increasing frequencies due to the increasing rate of electric field reversal. The polarization due to charge accumulation decreases, which leads to a decrease in values of ε' and ε'' [35].

Modulus analysis

The further analysis of the dielectric behaviour would be achieved by the dielectric moduli formulation, which suppresses the effect of the electrode polarization [36]. Electric modulus M^* is defined in terms of the reciprocal of the complex relative permittivity ε^* , i.e.

$$M^* = 1/\varepsilon^* = M' + M'' \quad (15)$$

The real and imaginary parts of the modulus for the NCPBEs prepared using both the methods viz., conventional mechanical stirring and the ultrasonic irradiation at different irradiation times are given in Fig. 5a–d.

At low frequencies, the real and imaginary parts of the modulus approach zero. This reveals that the electrode polarization phenomenon makes a negligible contribution. The long tail at low frequency is due to the large capacitance associated with the electrodes, which confirms the non-Debye behaviour nature of the system [37].

For all the filler concentrations, the shape of the spectrum remains constant, but the position of the peak maximum is shifted to higher frequencies for the 6 wt% filler concentration and to lower frequencies for the rest of the system prepared through the conventional mechanical stirring. Similarly, the position of the peak maximum is shifted to higher frequency for the system PEO–P(VdF–HFP)–LiClO₄–TiO₂ (6 wt%) at an optimum ultrasonic irradiation time of 10 mins, while for the other durations, the peak maximum is in the lower frequency side. This behaviour suggests that the relaxation peak

Table 5 Dielectric parameters σ_0 , A , n , ω_p , ε' , β and τ of the NCPBE subjected to ultrasonic irradiation

Sample name	σ (S cm ⁻¹) (from cole–cole plot)	σ_0 (S cm ⁻¹) (from Jonscher's power law fit)	A	n	ω_p	ε' (at 1 KHz)	β	τ (s)
TiO ₂ (6 wt%) ultrasonic irradiation time of 10 mins	2.270×10^{-4}	1.146×10^{-4}	4.885×10^{-6}	0.359	6.562×10^3	89.904	0.712	5.202×10^{-6}

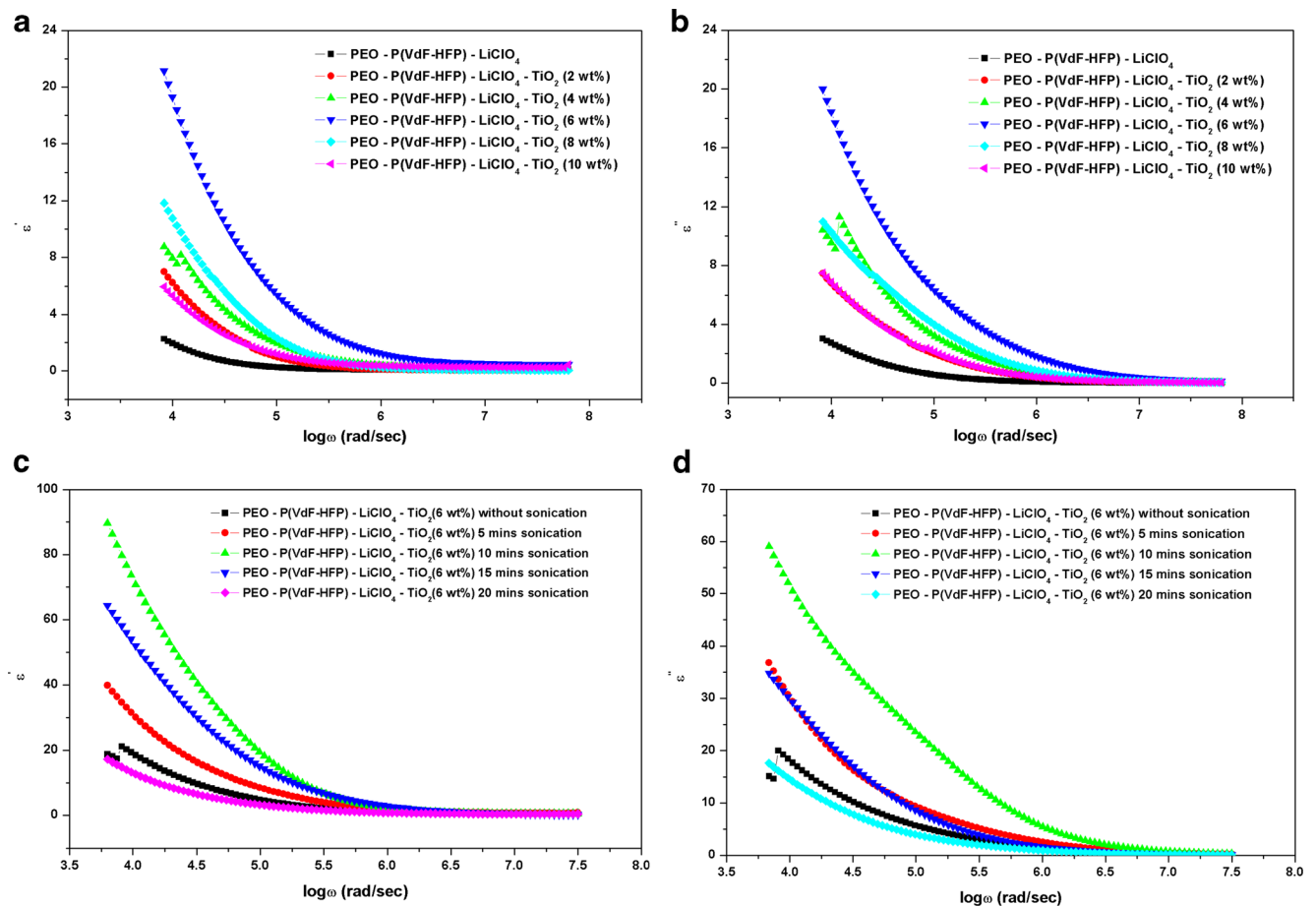


Fig. 4 **a** and **b** Frequency dependence of the dielectric constant ϵ' and dielectric loss ϵ'' for the prepared NCPBEs (conventional mechanical stirring). **c** and **d** Frequency dependence of the dielectric constant ϵ' and

dielectric loss ϵ'' for the system PEO–P(VdF-HFP)–LiClO₄–TiO₂ (6 wt%) at different ultrasonic irradiation times

is activated and charge carrier hopping is taken place due to both the addition of nano TiO₂ and also due to the ultrasonic irradiation.

The broad and asymmetrical shape of electric modulus is generally described by the stretched exponential function of the electric field as [38]

$$\varphi(t) = \exp\left[-(t/\tau)^\beta\right] \tag{16}$$

where $0 < \beta < 1$ is an exponent indicating departure from the Debye relaxation ($\beta=1$) and τ is the relaxation time. The parameter β for the samples are calculated using the formula $\beta=1.14/\text{FWHM}$ and are listed in Tables 4 and 5. From the tables, it is noticed that the values of β does not vary significantly and is lesser than one which suggests a greater departure from Debye relaxation. These lower values of β also suggest co-operative motion of the ions in the electrolytes, i.e. the jump of a mobile ion cannot be treated as an isolated event. In other words, the jump of the ions from one equilibrium site to another causes a time-dependent movement of other ions in the surroundings [39].

Tangent loss

Variations of tangent loss with a frequency of the NCPBEs are shown in Fig. 6a, b. The loss spectra of the samples showed a broad peak at a characteristic frequency which confirmed the presences of relaxing dipoles in the polymer composite electrolytes. The maximum of $\tan\delta$ shift towards higher frequency is due to the addition of TiO₂. It is noted that the 6 wt% of TiO₂ added system showed a shift in the higher-frequency side while the rest of the systems in the low-frequency side which are prepared by conventional mechanical stirring. On the other hand, the samples prepared using ultrasonic irradiation technique showed a high-frequency shift only for the optimum irradiation time of 10 mins and the other irradiation time showed a lower-frequency shift; as a result, segments of the polymer chains get more relaxed, thereby, the free volume of the complexes enhanced, hence more dipole relaxation is obtained which means that the shift towards the lower-frequency side suggests that the polymer chain segments get more relaxed, which in turn produces more free volume and results in more dipole relaxation [40], whereas the shift

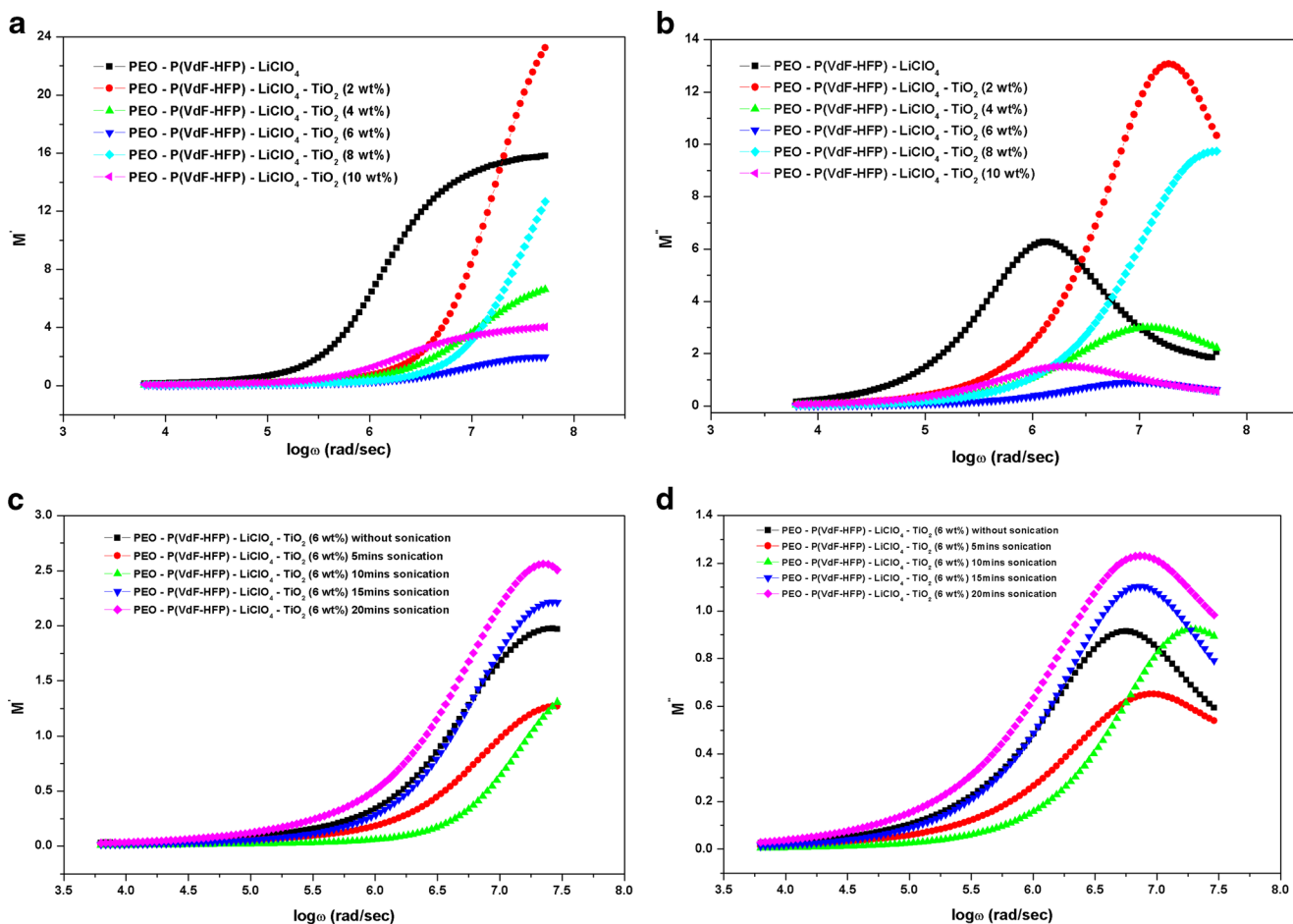


Fig. 5 **a** and **b** Real and imaginary parts of the electric modulus for the prepared NCPBEs (conventional mechanical stirring). **c** and **d** Real and imaginary parts of the electric modulus for the system PEO–P(VdF-HFP)–LiClO₄–TiO₂ (6 wt%) at different ultrasonic irradiation times

towards the higher-frequency side is attributed to fast segmental motion coupled with the mobile ion. Thus, both the addition of nano TiO₂ and the optimum ultrasonic irradiation time enhanced the amorphous region of polymer electrolytes. As the peak shifts towards the higher-frequency side, the

relaxation time is reduced. The relaxation parameters of the systems are given in Tables 4 and 5, which reveal that the relaxation time is lower for the sample with 6 wt% of nano TiO₂ system when compared with the samples having other concentration of nanofillers. The relaxation time gets further

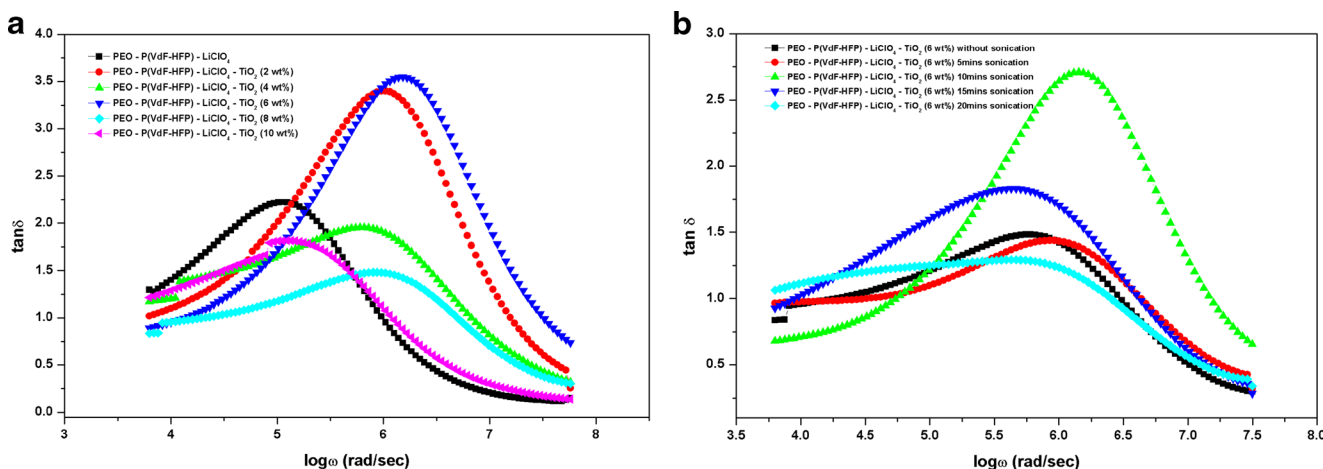


Fig. 6 **a** Variation of loss tangent with frequency for the prepared NCPBEs (conventional mechanical stirring). **b** Variation of loss tangent with frequency for the system PEO–P(VdF-HFP)–LiClO₄–TiO₂ (6 wt%) at different ultrasonic irradiation times

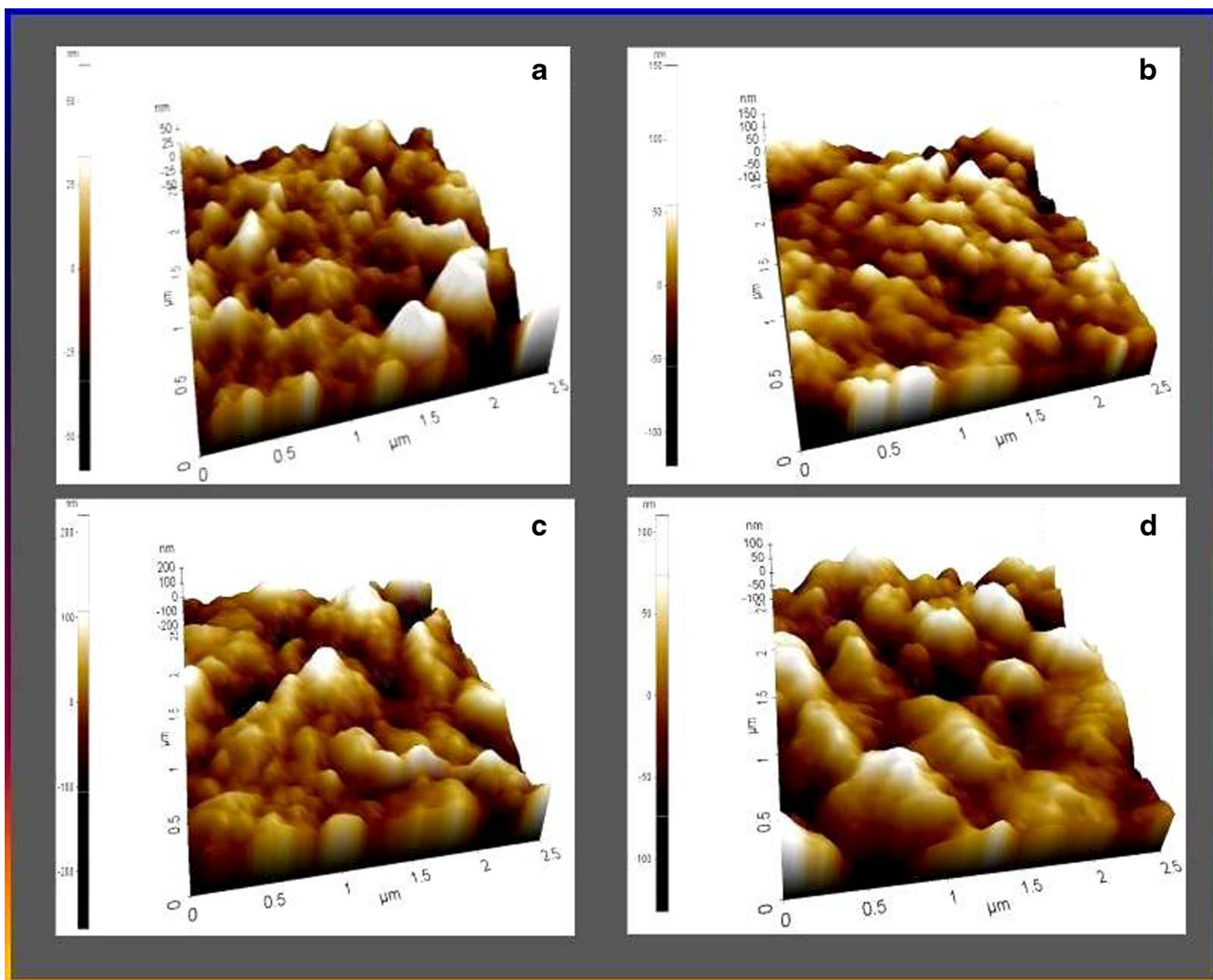


Fig. 7 AFM micrographs of **a** PEO–P(VdF–HFP), **b** PEO–P(VdF–HFP)–LiClO₄, **c** PEO–P(VdF–HFP)–LiClO₄–TiO₂ (6 wt%) (conventional mechanical stirring), **d** PEO–P(VdF–HFP)–LiClO₄–TiO₂ (6 wt%) (ultrasonic irradiation time of 10 mins)

reduced when the system is ultrasonically irradiated for 10 mins. These results are well close in agreement with the conductivity analysis.

AFM studies

AFM was used in tapping mode to study the morphological property of the nano TiO₂ filled polymer blend electrolytes. Three-dimensional surface plots of the polymer blend electrolytes are shown in Fig. 7a, b. Topographical images of the electrolytes prepared by conventional mechanical stirring and ultrasonic irradiation method are shown in Fig. 7c, d. A well-defined mountain-valley pattern with a roughness (RMS) value of 24.159 nm is observed for the surface of PEO–P(VdF–HFP) blend system (Fig. 7a). The polymer blend electrolyte, PEO–P(VdF–HFP)–LiClO₄, also shows a clear mountain-valley pattern (Fig. 7b) as observed for the blend but with more number of mountains and valleys. The

roughness value, 75.713 nm, of the polymer blend electrolyte is being higher than that of polymer blend (24.159 nm). This

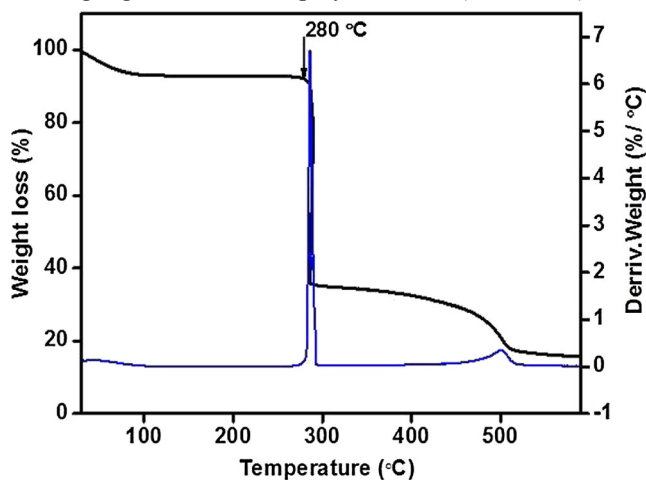


Fig. 8 TG/DTA thermogram of the sample PEO–P(VdF–HFP)–LiClO₄–TiO₂ (6 wt%)

increase of roughness value for the polymer blend electrolyte over the polymer blend suggests that there is good complexation between polymer blend and the salt used. The AFM micrograph of TiO₂ added polymer blend electrolyte prepared through conventional mechanical stirring (Fig. 7c) shows a definite morphological change when compared to that of the TiO₂ free polymer blend electrolyte (Fig. 7b). Again, an increase of roughness value (116.547 nm) is observed for the TiO₂ added system over the TiO₂ free system (75.173 nm). It can be inferred that the addition of TiO₂ has led to the structural modification of the polymer blend electrolyte.

Figure 7d is the AFM micrograph of TiO₂ added polymer blend electrolyte prepared through optimum ultrasonic irradiation. It also shows a well-defined mountain-valley pattern, with an increased surface roughness value as 133.671 nm. This confirmed the enhancement of amorphicity of the system due to the ultrasonic irradiation and hence supported the ionic transport.

TG/DTA analysis

TG/DTA analysis of the sample exhibiting a higher ionic conductivity is shown in Fig. 8. From the TGA curve, it was noted that the sample T3 showed a thermal stability about 280 °C. It was also noticed that there was a small valley originated around 100–110 °C which may be due to the removal of residual solvent present in the sample or by the absorbance of the moistures during the sample preparations [41]. The obtained TGA result was also well correlated with the DTA results. The huge weight loss of the sample started at 280 °C was confirmed by the exothermic peak which implies the usage thermal region of the sample.

Conclusion

Nanocomposite polymer electrolytes composed of PEO-PVdF-HFP-LiClO₄ were prepared for various concentrations of TiO₂ nanofiller. It was noted that the ionic conductivity increased by increasing the filler content, and the complex containing 6 wt% showed a maximum ionic conductivity about 1.451×10^{-5} S cm⁻¹. The composite polymer electrolytes were also subjected to ultrasonic irradiation for further improving the conductivity; it was noted that the sample containing 6 wt% irradiated about 10 mins exhibited a higher ionic conductivity value about 2.270×10^{-4} S cm⁻¹. Surface morphology of the samples was studied using AFM analysis. Thermal stability of the sample exhibiting higher ionic conductivity was determined from TG/DTA analysis. Thus, from the obtained analysis, it was clearly noted that the polymer

electrolytes met the required electrical properties; hence, it can be used as electrolyte in the possible device fabrications.

References

- Ramesh S, Ling OP (2010) *Polym Chem* 1:702
- Sim LN, Majid SR, Arof AK (2012) *Solid State Ionics* 209–210:15
- Staiti P, Lufitano F (2010) *Electrochim Acta* 55:7436
- Ghosh A, Kofinas P (2008) *ECS Trans* 11:131
- Kovac M, Gaberscek M, Grdadolnik J (1998) *Electrochim Acta* 44:863
- Jacob MME, Hackett E, Giannelis (2003) *J Mater Chem* 13:1
- Ahmad Z, Al-Awadi NA, Al-Sagheer F (2007) *Polym Degrad Stab* 92:1025
- Rajendran S, Kesavan K, Nithya R, Ulaganathan M (2012) *Curr Appl Phys* 12:789
- Ulaganathan M, Nithya R, Rajendran S, Raghu S (2012) *Solid State Ionics* 218:7
- Derrien G, Hassoun J, Sacchetti S, Panero S (2009) *Solid State Ionics* 180:1267
- Chakrabarti A, Juilfs A, Filler R, Mandal B (2010) *Solid State Ionics* 181:982
- Joykumar Singh T, Bhat SV (2009) *J Power Sources* 129:280
- Ravi M, Pavani Y, Kiran Kumar K, Bhavani S, Sharma AK, Narasimha Rao VVR (2011) *Mater Chem Phys* 130:442
- Ulaganathan M, Rajendran S (2010) *Ionics* 16:667
- Johan MR, Shy OH, Ibrahim S, Yassin SMM, Hui TY (2011) *Solid State Ionics* 196:41
- Zhang J, Han H, Wu S, Xu S, Zhou C, Yang Y, Zhao X (2007) *Nano Technol* 18:295606
- Klein RJ, Zhang S, Dou S, Jones BH, Colby RH, Runt R (2006) *J Chem Phys* 124:144903
- Chandra A, Chandra A, Thakur K (2012) *Port Electrochim Acta* 30:81
- Baskaran R, Selvasekarapandian S, Kuwata N, Kawamura J, Hattori T (2007) *J Phys Chem Solids* 68:407
- Michael MS, Jacob MME, Prabakaran SRS, Radhakrishna S (1997) *Solid State Ionics* 98:167
- Tsunemi K, Ohno H, Tsuchida E (1983) *Electrochim Acta* 28:833
- Saikia D, Chen-Yang YW, Chen YT, Li YK, Lin SI (2008) *Desalination* 234:24
- Chiang CY, Shen YJ, Jaipal Reddy M, Chu PP (2003) *J Power Sources* 123:222
- Nookala M, Kumar B, Rodrigues S (2002) *J Power Sources* 111:165
- Druger D, Nitzan A, Ratner MA (1985) *Phys Rev B* 31:3939
- Cowie JMG, Spece GH (1998) *Solid State Ionics* 109:139
- Johnscher AK (1977) *Nature* 267:673
- Natesan B, Karan NK, Katiyar RS (2006) *Phys Rev E* 74:0420801
- Hirankumar G, Selvasekarapandian S, Bhuvaneshwari MS, Baskaran R, Vijayakumar M (2006) *J Solid State Electrochem* 10:193
- Siekierski M, Wiczorek W, Przulski J (1998) *Electrochim Acta* 43:1339
- Nithya H, Selvasekarapandian S, Arunkumar D, Sakunthala A, Hema M, Christopherselvin D, Kawamura J, Baskaran R, Sanjeeviraja C (2011) *Mater Chem Phys* 126:404
- Reicha FM, El-Hiti M, El-Sonabati AZ, Diab MA (1991) *J Phys D Appl Phys* 24:369
- Campbell JA, Goodwin AA, Simon GP (2001) *Polymer* 42:4731
- Balaya P, Goyal PS (2005) *J Non-Cryst Solids* 351:1573
- Ibrahim S, Yassin SMM, Ng Meng N, Ahmad R, Johan MR (2012) *Solid State Commun* 152:426

36. Ramesh S, Arof AK (2001) Mater Sci Eng B 85:11
37. Muralidharan P, Venkateswarlu M, Satyanarayana N (2005) J Non-Cryst Solids 351:583
38. Hodge IM, Ngai KL, Moyinhan CT (2005) J Non-Cryst Solids 351:104
39. Reau JM, Rossignol S, Tanguy B, Rojo JM, Herrero P, Rojas RM, Sanz J (1994) Solid State Ionics 75:65
40. Agrawal SL, Singh M, Tripathi M, Dwivedi MM, Pandey K (2009) J Mater Sci 44:6060
41. Ulaganathan M, Rajendran S (2010) Ionics 16:515